Uncertainty Minimization and Pattern Recognition

in *Volvox Carteri* and *Volvox Aureus*

Franz Kuchling[1], Isha Singh[1], Mridushi Daga[1], Susan Zec[1], Alexandra Kunen[1], Michael Levin[1]*

[1]Allen Discovery Center, Tufts University, Medford MA (US)

*Corresponding Author. Michael.Levin@tufts.edu

Keywords: *Volvox*, surprise, minimal cognition, diverse intelligence, algae

Running title: Uncertainty minimization in algae

Abstract

Learning and a spectrum of other behavioral competencies allow organisms to rapidly adapt to dynamically changing environmental variations. The emerging field of diverse intelligence seeks to understand what systems, besides ones with complex brains, exhibit these capacities. Here, we tested predictions of a general computational framework based on the free energy principle in neuroscience but applied to aneural biological process as established previously, by demonstrating and manipulating pattern recognition in a simple aneural organism, the green algae *Volvox*. Our studies of the adaptive photoresponse in *Volvox* reveal that aneural organisms can distinguish between patterned and randomized inputs and indicate how this is achieved mechanistically. We show that the phototactic response in *Volvox* adapts more readily to regular light pulse patterns than to irregular ones, thus exhibiting a crucial component of basal intelligence - generalization: the ability to recognize patterns in input stimuli. Randomized electric shocks reduced the ability of *Volvox* to maintain adaptive phototaxis significantly more than regularly applied electric shocks, providing first evidence for a stress effect of randomized input patterns in a primitive organism. Moreover, we detected memory in *Volvox* - a persistence of movement towards past light stimulation through their phototactic orientation, another foundational aspect of neural-like primitive cognition. Combined, these data reveal that *Volvox* exhibit a capacity for pattern recognition consistent with uncertainty minimization. The ability of algae to be surprised and distinguish random events that do not meet expected patterns further expands neurobiological concepts beyond neurons. These methods can likely be translated to the study and manipulation of basal cognition in many other living systems.

1 Introduction

Living organisms are good at detecting, responding to, and adapting to variable environments, not just on evolutionary time-scales, but also via short- and long-term adaptive organismal behavior. Interestingly, this does not require brains or advanced nervous systems [1-4] . Examples of learning and adaptive behavioral responses in aneural organisms include context-dependent motility [5, 6], stress response-triggered learning [7, 8], anticipation [8], long range spatial decision-making [9], and associative learning [10] in a range of microbial organisms. Even Embryophytes, despite their apparent lack of dynamic motility, possess highly complex adaptive responses through their fast and complex internal calcium signaling patterns [11]. Similarly, in vascular plants, synaptic adhesions domains and action potentials [12, 13], yield self-identity and recognition capabilities through their use of plant-specific synapses in *Cayratia japonica* [12], and can detect acoustic vibrations from feeding caterpillars and subsequent elicitation of chemical defenses in *Arabidopsis thaliana* [14]. Furthermore the slime mold Physarum detects materials properties of its environment via pulsatile mechanosensing and makes growth decisions based on information gleaned about objects at long range [9].

The ability to detect environmental patterns and distinguish them from random noise is considered a basic component of intelligence – the inference of a general pattern from particular experiences. Such a pattern can serve as the primitive basis of counterfactuals, because the recognition of a pattern endows an organism with expectations for what should happen next, before it happens. While ubiquitous seasonal and day-night cycles provide a highly reliable environmental pattern which is constant across generations (and thus can serve as a stable target for selection), it is unclear how much individual aneural organisms can detect and adapt to novel and more variable patterns on much shorter timescales. Our work was motivated by two inter-related questions: How far down the evolutionary scale of complexity do organisms exhibit the ability to detect novel environmental patterns, and do they have

expectations that may or may not be met? What frameworks can help us understand these capacities in novel substrates?

Changes in a cell's extracellular environment can affect both its current physiological states and its future states, both physiological and genetic. An example of environmentally triggered immediate changes in current cellular active states is seen in basic phototactic organisms, where light-induced protein conformation states coupled to changes in flagellar beating rates result in movement towards or away from light stimuli. The short-term changes in light sensitivity and downstream flagellar beating responsivity that are the core of this ability to orient towards light and maintain direction are referred to as photoadaptation [15]. While the mechanisms of delayed adaptive responses of light-sensitive cells are fairly well-understood in the human visual system as being mediated through intracellular signaling coupled to transcription, translation, and epigenetic modifications, photoadaptation has not been well studied in simpler phototactic organisms such as *Volvox*.

Work over the last decade has shown that patterned environmental stimuli that differ only in the frequency of presentation to the organism, can elicit distinct downstream signaling events and functional (behavioral) outcomes in many kinds of cellular systems. For example, Mitchell et al. varied osmotic concentrations over time in pulsatile fashion and identified a frequency-specific activation and refractory relationship in the MAPK pathway that inhibits yeast growth severely, but only at specific frequencies of osmotic oscillation [16]. The use of optogenetics to dynamically activate signaling pathways has been a significant contributor to further understanding the mechanistic basis for this ability [17]. A prominent example comes from the Toettcher group, which used optogenetic activation of EGF to vary the temporal dynamics of ERK signaling and showed that temporal variation in activation pulse frequency induction of ERK signaling not only affects the amount of transcription and subsequent translation of a target gene, but can also trigger transcription of different target genes [18, 19].

Physiological bottom-up models employed in the examples above require a high degree of detailed knowledge of the underlying mechanistic biochemical pathway activation and require a high degree of experimental accessibility to those molecular pathways to be useful, which is not always

possible. Thus, here we aimed to understand these phenomena from a top-down perspective focusing on the response of the system to patterns and information content in its environment - by generalizing a theoretical framework of adaptive responses to dynamic inputs reminiscent of higher-level information processing common to many cellular systems. Using a cognitive Bayesian framework based on our earlier work [20] and that of Karl Friston and others in the field [21-26] , we can formulate a model of cellular beliefs (or predictions) that encode what type of signals the cell expects to receive at any given point in time. These cellular beliefs encompass all the receptors and cellular machinery currently expressed and represent the cell's best estimate of which physiological and transcriptional state will make it the most adaptable to current and anticipated environmental effects [20, 27]. Regulatory output aimed at modifying the signaling activity could hence be interpreted as the effort to minimize uncertainties in measurements of the environment compared to expected signaling inputs. Mechanistically, cellular expectations for input signaling activity stem from the state of the internal signaling pathway dynamics of the cell, itself encoded by transcriptional dynamics (with changes occurring in the range of minutes to hours) on the one hand, but also by more short-term state changes in protein conformations (e.g., opening and closing of ion channels and activation and internalization of receptor proteins) and activity profiles (ion inflow, propagation and available storage, such as encompassed through calcium dynamics) on the other. The ensuing transcriptional outputs and functional changes of proteins realize a constant modification of physiological and biophysical parameters affecting signaling transmission.

The uncertainty minimization employed by the cells as dictated by Bayesian inference [20] predicts that random (and hence unpredictable) dynamic stimulation will elicit a stronger but less directed cellular physiological and transcriptional response than a regular, predictable dynamic stimulation, resulting in an aversion to irregular environments and preference for more regular ones [28]. Specifically, this idea has been developed in a rich body of work on surprise minimization [22, 24, 29-31] which emphasizes the drive of living beings to continuously improve their internal models of their environments and of themselves. These ideas are frequently discussed with respect to neural brain mechanisms; however, given the wide conservation of signaling mechanisms and algorithms across

neural and non-neural cells [32, 33], it becomes especially interesting to ask whether systems with no brains, and no neurons, can likewise support expectations about the future born of pattern inference, and exhibit responses which reveal that these expectations cannot be met in random environments.

Here, we test the hypothesis that aneural organisms can display actionable pattern recognition in general and uncertainty minimization in particular. We chose to investigate this using the photoadaptive response in two different subspecies of the chlorophyte green algae *Volvox* (*Volvox carteri* and *Volvox aureus*) as a readily measurable adaptive behavior to an external physical stimulus that can be varied in any temporal pattern. We simulated different light stimulation patterns (including crucially randomized ones) in our model and tested their predictions for variable effect on phototactic modulation in *Volvox*. We designed an experimental platform that allows us to compare *Volvox* phototaxis towards two distinct regimes of light stimuli with different patterns of light pulsation, exploring mechanisms and long-term effects on the organism. We complement the phototactic trajectories obtained from these experiments with gain-of-function drug experiments focused on shifting phototactic biases based on both our knowledge of underlying molecular pathways and their effect on their information processing modalities. We furthermore also tested whether *Volvox* exhibit short-term memory towards past light stimuli in terms of their phototactic paths, which would provide them with further crucial neural-like capabilities. We also tested whether *Volvox*' photosynthesis would also be affected by dynamic light patterns in an attempt to detect metabolic manifestations of uncertainty minimization in *Volvox*. Finally, to begin exploring the potential for training of *Volvox* photoaxis to desired light pattern biases, we examined whether patterned electric shocks could *manipulate Volvox* responses to patterned light stimuli. Taken together, our results reveal capacities which would not normally be expected in algae and provide a proof-of-concept for searching for such capacities in a wide range of minimal and synthetic model systems.

2 Methods

2.1 Culture Conditions and Strains

Volvox carteri eve strain (female) was obtained from Bradley J. S. C. Olsen Lab and grown in either grown in Standard *Volvox* Media (SVM) or AlgaGro®. Both strains are incubated in a Peltier cooled incubator (catalogue number 3915FL) at 30C under a 14-hour light and 10-hour dark cycle (Jiménez-Marín et al, 2021). A 75W LED Grow Panel (model number HY-MD-D169-S-75W-RB-US) was used inside the incubator to maintain the light and dark cycle. SVM media is prepped following previously tested recipe by the Olson lab (2017). AlgaGro® medium is purchased in 50x concentrate form from Carolina (catalog number 153758) and diluted in Poland Spring water per instructions from the manufacturer. Every time new *Volvox* are used for experiments, the entire culture flask is gently mixed and placed in front of a light source for at least 5 minutes to allow active *Volvox* to move to one side of the flask for easy collection of 1-2 milliliter of between 500 and 2000 viable *Volvox* colonies.

2.2 Light-Stimulation Apparatus and Imaging

Initial experiments with *Volvox aureus* were done in ABS plastic chambers printed by a Fused Deposition Modeling (FDM) 3D printer, with clear polystyrene plastic glued to the sides for light access.

Light Stimulation was achieved using standard through hole blue LEDs (from Mouser Electronics, catalog number 630-HLMP-CB1A-XY0DD) with a wavelength of 470 nm and an opening angle of 15 degrees, controlled with an LED driver from Thorlabs (part number: LEDD1B), dialed to power output 1mm from the LED of 2mW. To calibrate the LEDs to equal outputs, LEDs were pre-sorted to similar outputs, then soldered into a parallel circuit with a potentiometer in series with every individual LED. Then, light intensity was measured using a photometer probe at 2 distances, right at the LED and at 6cm away from it, after which angle of the LED and resistance of the potentiometer were adjusted to achieve a good match of intensities from row to row, as well as from side to side.

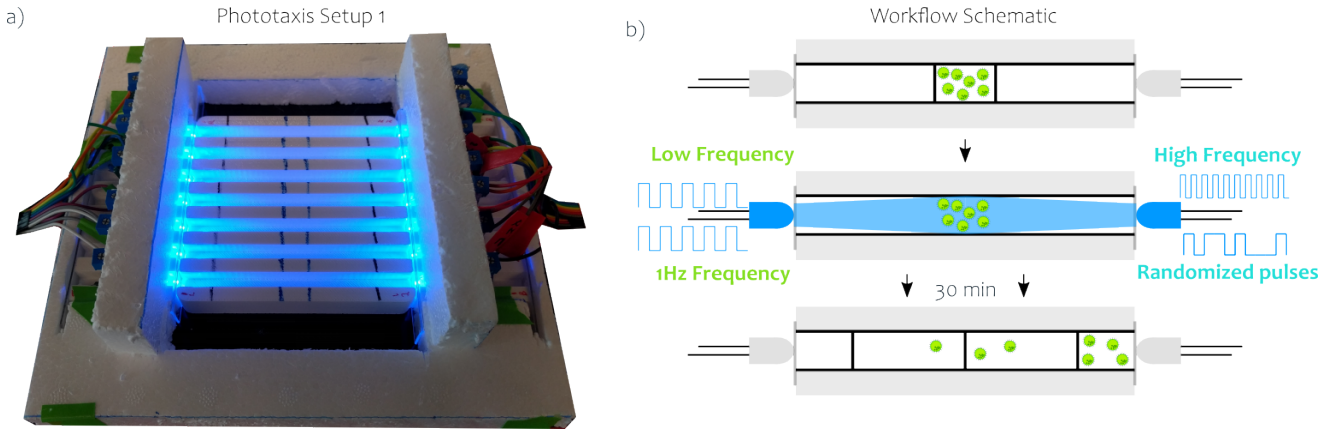

Figure 1. Apparatus and Workflow for Manual Counting of Phototactic Biases.
a) Phototaxis set-up. Blue LEDs (470nm) mounted to the side of 10cm long chambers illuminated the inside of the chamber with blue light. b) Experimental schematic. An average of 20-30 *Volvox* were inserted into the middle of each medium-filled chamber ('lane') using a pipette. The middle section of each lane was delimited from the rest of that lane by clear, watertight PDMS stoppers. Once all the *Volvox* were added, stoppers were removed from all lanes, and the light pulse series was started on both sides simultaneously. After 30 minutes, the program ended, at which point stoppers were inserted at the middle and end points, and the medium with *Volvox* was removed from each section and *Volvox* were counted under a microscope.

Quantification in this setup was achieved through collection of *Volvox* colonies in the different sections with subsequent manual counting using still images of the collected colony ensembles. Plots of phototactic biases using the setup shown in Figure 1 only consider the approximate position of *Volvox* in the end sections of the chambers which show a more pronounced bias due to the length of the chamber when compared to the second setup shown in Figure 2 which allows for less swimming back and forth of *Volvox*.

All light experiments performed on *Volvox carteri* used SK9822 individually addressable RGB LEDs. with total light outputs above the LED at 2mW each. Light patterns were programmed using Arduino Nano Controllers. Housings for adaptive cultures were printed with ventilation holes reaching from underneath upwards between LEDs and cultures flasks to aid in heat distribution. Phototactic experiments were performed with only the blue light from the LED at 460 nm, while growth experiments and oxygen measurements were performed at both blue and red (650 nm) light to match incubator conditions.

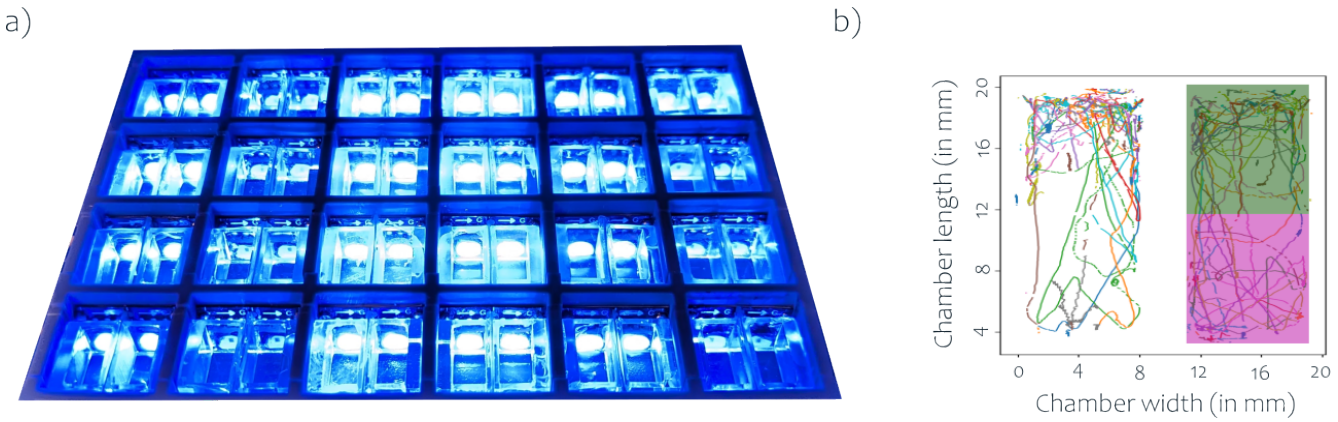

Figure 2. Apparatus and Workflow for Manual Counting of Phototactic Biases.
a) Individually controllable blue LEDs in 48 chambers were pulsed in different light. b) Quantification of *Volvox* phototactic bias was performed based on computational tracking of the images acquired with the MCAM camera array above the chamber. The different colors of the tracks indicate the swimming trajectories of individual *Volvox* colonies, while the shaded areas in green and magenta on the right indicate the two halves of the chambers closer to either of the two opposing light sources, such as a fixed 1 Hz light pulse frequency, color coded throughout this paper in green, versus a randomized light pulse sequence, color coded throughout this paper in magenta.

Using the MCAM Gigapixel Multi-Camera array of 24 cameras, up to 48 individual chambers (2 per camera) can be observed at high spatio-temporal resolution simultaneously with individual light pattern stimulation for each chamber.

3d printed clear dual chambers with an optically opaque divider inserted between the two chamber halves to reduce light contamination from the sides are inserted into the device for experiments with *Volvox* and are removable. Autofluorescence of *Volvox* was detected at peak wavelength of 695 nm using a near IR long pass filter a passthrough wavelength of 685 nm, where the excitation light was the blue light from the LED light at 460 nm.

2.3 Computational Tracking and Analysis

To analyze the movement of *Volvox*, a python (version 3.10) program was created that utilizes the trackpy library (version 0.4.2, https://soft-matter.github.io/trackpy/v0.4.2/) to track the particle trajectories. The program takes in multiple parameters including, but not limited to, the following: size, speed, and integrated light intensity of each *Volvox* colony, x and y midpoints of the chamber, and number of *Volvox* colonies. Additionally, the program can adjust for *Volvox* that are stationary during

most of the tracking, so that they can be counted separately for further analysis, or excluded in the counting analysis to remove *Volvox* that are stuck to a surface due to their flagella getting caught to imperfections on the chamber surface. As these imperfections have been reduced heavily by sanding and clear coating of the chambers, this only applies to a small proportion of *Volvox* and no bias towards different light patterns was observed, as the mechanism is unrelated to the light. The program then takes the filtered information and counts how many *Volvox* are in each half of the chamber.

2.4 Electric-Shock Treatment

2.4.1 Chamber Configuration

A 3d printed 30mm x 20mm x2mm chamber as shown above was resin printed. 0.5-millimeter (diameter) platinum iridium wire (catalog number AA10056BS) electrodes were inserted through holes printed on either side of the chamber allowing 1 millimeter of the electrode to be exposed within the active area of the chamber. An additional chamber stage was printed to act as a holder for a strip of LED lights. The lights were controlled through an Arduino microcontroller, with programs determining the intensity of light.

2.4.2 Voltage and Current Control

Initial voltage source used for preliminary, constant voltage testing was a DC laboratory DC power supply, model: GPS-1830D. This was strictly used as a voltage source, while the LED Driver was used to modulate current. For the LED driver (part number LEDD1B), the current limit was set at 0.2 Amps and dialed until the voltage in the chamber was measured at the desired level, then balanced with resistors in parallel to lower the actual current going through the chamber to non-destructive levels. Measurements were done using a multimeter. An Arduino Nano microcontroller was used to modulate the current.

2.5 Oxygen Measurements

We used the Firesting® apparatus from pyrotechnics, which measures oxygen concentration in a vial in gaseous or aqueous form by scanning an oxygen sensitive sensor spot inside the glass vial from the outside with an optical fiber probe. *Volvox* cultures were expanded 2 days before start of treatment into 4 flasks of 200 ml each, then, before start of treatment, combined in a conical tube, gently inverted to thoroughly mix the cultures, and then separated into 4 new flasks. One was left as control in the incubator, while the other 3 were exposed to light in dome-shaped 3d printed devices with inbuild LEDs with ventilation holes on the bottom, and open space towards the top of the culture flask, but shielding the culture flasks form the rest of the incubator lights during treatment. Oxygen measurements were taken before treatment, and then after 6, 24, 30, and 48 hours respectively by slowly and gently swirling each flask to mix the media but not to agitate and add more oxygen, then gently and extremely slowly transferring 5ml using a Pasteur pipette of one culture into the oxygen measurement vial with a temperature probe in it for temperature compensation of oxygen concentration measurement.

3 Results

3.1 *Volvox* Distinguish Between Patterned and Random Light Stimuli

To investigate the ability of *Volvox* to detect and differentially react to temporal light patterns, we designed 3D-printed chambers of different sizes, consisting of isolated channels with clear ends, each end illuminated by a separately microcontrolled LED, with manual counting (Figure 1) and camera-based tracking (Figure 2). Based on our central hypothesis of surprise minimization in aneural organisms, we tested the prediction that a phototactic organism such as *Volvox* would reveal a preference for order (or a dislike of unpredictability) by preferentially moving towards light stimulation patterns of higher regularity (and hence predictability). When we exposed *Volvox* to an overall equal amount of light over time but at a regular, fixed light pulse interval versus a randomized, irregular light pattern (see Figure 3), a significantly larger proportion of *Volvox aureus* were detected in the section adjacent to the fixed interval stimulation than in the section adjacent to the random stimulation ($p<0.05$, Wilcoxon signed-rank test), in accordance with our predictions based on uncertainty minimization.

Because of this observed preferential movement of *Volvox aureus* to the regular 1 Hz light pattern when opposed with a randomized light pulse pattern of similar average pulse length, we conclude that *Volvox* can distinguish patterned light stimuli from random ones, a fundamental building block for intelligent information processing [34, 35].

To minimize sources of error and bias from manually counting *Volvox* and to get real-time data on *Volvox* photoadaptation for downstream data-mining, we also designed and tested a system that combines highly transparent smaller chambers (reducing the effect of light scattering) with a high-resolution camera system. We used this apparatus to test the same hypothesis on another species of *Volvox, V. carteri*, which is evolutionarily distant from *V. aureus* by an estimated 75 million [36].

Our results in this automated platform show that, as for *V. aureus*, *V. carteri* also exhibits a photoadaptive bias towards a regular light pulse pattern vs. a random one (see Figure 3a), as over time, more *Volvox* swam closer to the patterned stimulus side than to the randomized stimulus side ($p<0.01$).

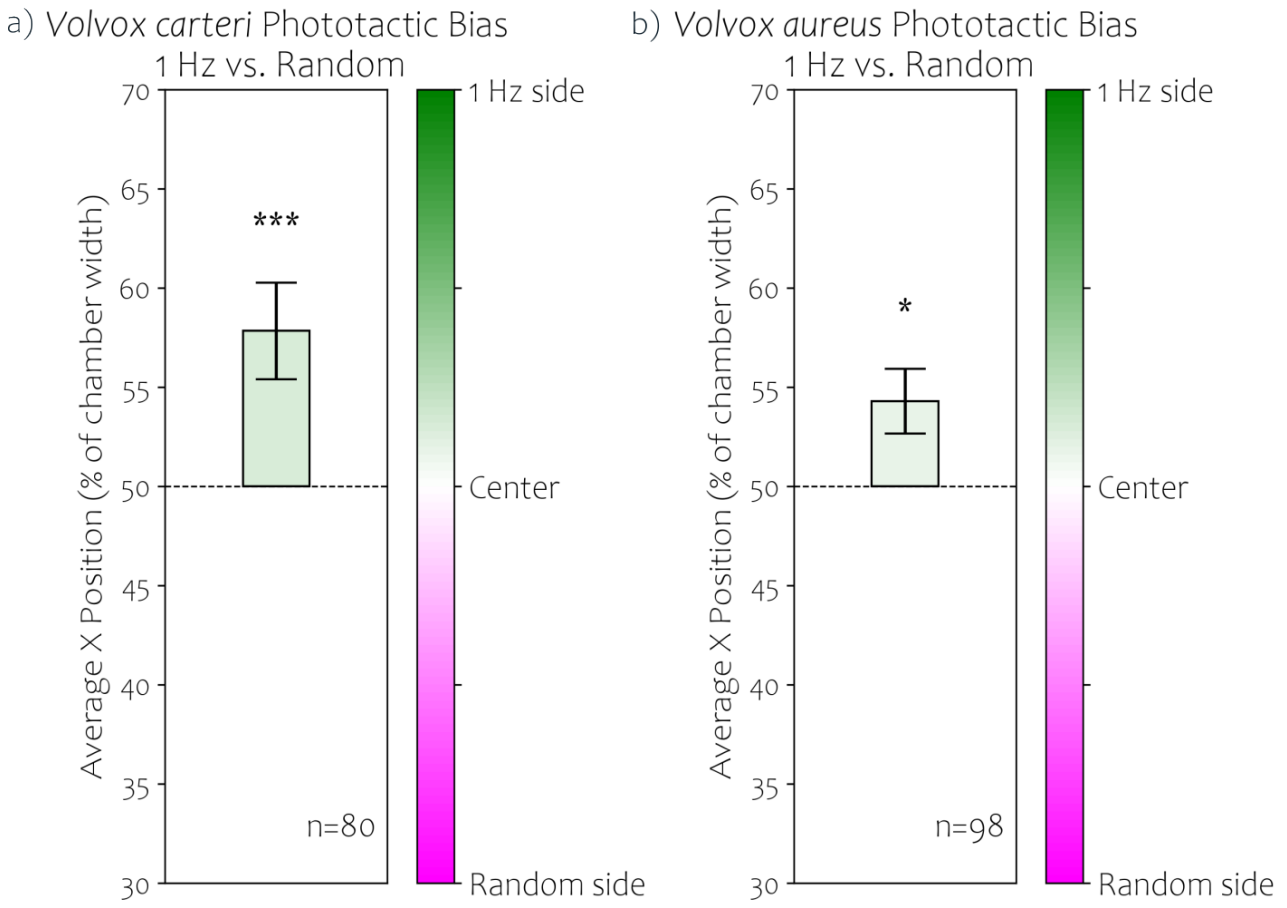

Figure 3. Photoadaptation in *Volvox carteri and aureus* Exhibits as Bias Against Randomized Light Pulses.
Volvox carteri and *aureus* prefer fixed (1Hz, 0.5s light duration) over random light pulse series.
a) *Volvox carteri* phototactic bias was quantified as indicated in Figure 2. Plotted are the average x (along the major axis of the chamber) position in percent relative to the chamber width for each experiment. (*** indicates $p<0.001$, Wilcoxon signed-rank test).
b) Phototactic preference in *Volvox aureus* was measured by counting of *Volvox* colonies that were collected in one end of the well versus the other (see Figure 2), after which average x position was approximated in the same manner as in a). A significantly larger proportion of *Volvox aureus* was detected in the section closer to the fixed interval stimulus than the randomized stimulus. (* indicates $p<0.05$, Wilcoxon signed-rank test).

We exploited the detailed quantitative nature of this imaging apparatus to investigate the influence of *Volvox* colony size (µm), swimming speed and the number of colonies inside the chamber on its phototactic bias using a Principal Component Analysis (PCA) analysis. The PCA revealed that the first two principal components accounted for 91.07% of the total variance in the data, with PC1 explaining 56.72% and PC2 explaining 34.35%. The third component, PC3, accounted for the remaining 8.94% of the variance. The component loadings for each variable are presented in Table 1.

Variable	PC1	PC2	PC3
Colony Size	0.941450	0.064707	0.365889
Swimming Speed	0.900969	-0.298521	-0.351469
# of Colonies	-0.212085	-0.980930	0.131096

Table 1: PCA Component Loadings

PC1, explaining the majority of the variance (56.72%), showed strong positive loadings for both *Volvox* colony size and swimming speed. PC2, accounting for 34.35% of the variance, was predominantly characterized by a strong negative loading for the number of colonies per frame.

The strong positive loading for both *Volvox* colony size and swimming speed in PC1 suggest a robust positive correlation between these two variables, indicating that larger *Volvox* colonies tend to swim at higher speeds in our system. This relationship could be attributed to the increased propulsive force generated by larger colonies with more flagellated cells. The strong negative loading for the number of colonies per frame in PC2 suggests that this component appears to represent colony density, largely independent of size and speed. The moderate negative loading for speed on this component suggests a slight tendency for lower swimming speeds in frames with higher colony counts, possibly due to increased hydrodynamic or direct flagellar interactions, leading to *Volvox* colonies getting stuck to each other temporarily. PC3, while only explaining 8.94% of the variance, revealed an interesting contrast between colony size and swimming speed. This minor component might capture exceptions to the main trend, possibly representing scenarios where larger colonies move more slowly or smaller colonies move more quickly and could be related to variations in colony morphology, flagellar activity, or local environmental conditions. The high cumulative variance explained by PC1 and PC2 (91.07%) indicates that the three-dimensional data can be effectively represented in two dimensions with minimal loss of information. This suggests a strong underlying structure in the *Volvox* population dynamics, primarily driven by the size-speed relationship and variations in colony density.

Based on this analysis, we filtered *Volvox* by size (colony diameter between 120 and 150μm) and swimming speeds (larger than 120 μm/s) for higher uniformity and standardization of our data. Thus, the

most effective distinction between the random and patterned stimuli was being carried out by *Volvox* of that size and swimming speed.

3.2 *Volvox* Show Optimal Photoadaptation to Specific Frequencies

We next examined which light pulse frequencies, if any, *Volvox* most readily adapt to — by exposing *Volvox* inside the channel to different light pulse frequencies on each side of the chamber. We tested various pulse frequencies from 50Hz to 1Hz and determined the percent of *Volvox* that swam to each end of the chamber (see Figure 4). There was a clear preferential adaptive response to light pulse frequencies of 2 Hz when opposed to smaller and larger pulse frequencies respectively ($p<0.001$ as determined by Wilcoxon signed-rank test). From this we conclude that *Volvox* distinguish different regular patterns in terms of their adaptive, phototactic response.

Using the automated tracking apparatus, we also tested the presence of a phototactic biases in *Volvox carteri* for the highly significant case of 1 Hz vs. 2 Hz in *Volvox* aureus. However, unlike in *V. aureus* (see Figure 4), in *V. carteri* there was no difference between photoadaptive responses to either opposing light stimuli of 1 and 2 Hz respectively. We only compared two frequencies, so it is very possible that photoadaptation in *V. carteri* is optimized to a different frequency range than in *V. aureus*, possibly due to a slightly different flagellar response times or an overall rotational speed difference compared to *V. aureus*. These differences would need to be investigated in future studies, as no such detailed studies have been done in *Volvox aureus*.

The data from section 3.1 on the patterned vs. randomized light sequences, combined with these data on different light pulse frequencies in two similarly simple aneural species, support the hypothesis that even aneural organisms can detect patterns and tend to avoid random stimulation patterns precisely because of the difference in overall predictability of those stimulation patterns, and not just due to differences in frequency.

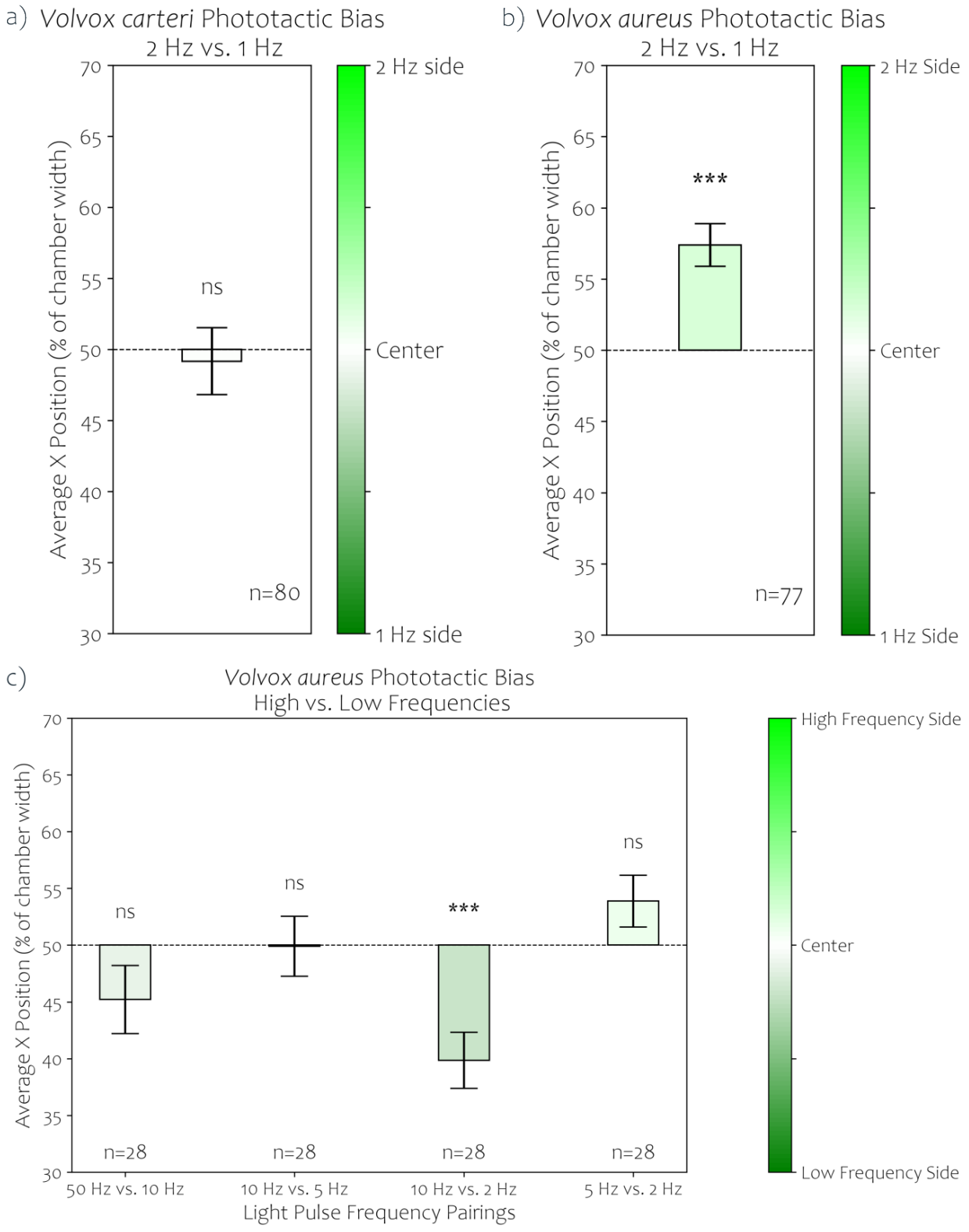

Figure 4. Photoadaptation in *Volvox aureus* and *carteri* is Optimized for Different Specific Light Frequencies.

a) No significant phototactic bias was observed between 1 Hz vs. 2Hz stimuli for *V. carteri.* b) For *V. Aureus* however a very significant (*** indicates $p<0.001$, Wilcoxon signed-rank test) bias was observed towards the 2 Hz side, indicating a difference in photoresponse between the 2 species. c) Different light pulse frequency pairings reveal a lack of biases in frequencies higher and lower than 1-2 Hz, while a stronger bias towards 2 Hz was observed against 10 Hz, indicating a window of optimal photoadaptation in *V. Aureus* towards 2Hz.

3.3 Simulation Using a Cellular Scale *in silico* Model of *Volvox* Response to Random vs. Patterned Inputs Predicts that Uncertain Inputs Decrease Photoadaptation

In order to probe how uncertainty minimization is implemented mechanistaically on a physiological level, we built on work by Drescher et al. [15], to simulate the adaptive phototactic response of *V. carteri* to the same types of input used in our experimental system above (Figures 1,2). We simulated flagellum beating speed downregulation in response to inputs reflecting fixed vs. randomized light pulse stimulations with similar average interval length and equal total light exposure. The average adaptive or recovery time (the time it takes for a flagellum to return to baseline beating frequency after photostimulation) obtained for the irregular, randomized light input series was greatly reduced (see Figure 5e). This was evidenced by the reduced time it took for simulated fluid speed induced by flagellar beating to return towards baseline following the random pulse sequence compared to the fixed pulse sequence (Figure 5c). Given the ubiquity of Poisson distributed neuronal activation patterns in neural organisms [37], we confirmed that when we randomized inputs by shuffling stimulation pulses (which constrained each stimulation to yield similar average pulse duration and equal total light exposure), the histogram of inter-pulse durations exhibited a Poisson distribution (see Figure 5f), which is the distribution most used to model natural pulsed stimulation patterns in human brains [37] to avoid adaptation through habituation to repeated stimuli. As seen below, this opens up research on short term adaption in *Volvox* as a foundation for learning, as Poisson type stimulation patterns have been shown to evoke distinct spike timing dependent plasticity (STDP) in neurons [38]. In other words, neural systems react very different to purely random Poisson distributed spike trains versus tightly regulated, repeatable activation patterns, the balance thereof being an active source for debate and likely varies in different neuronal systems depending on how tightly information is compressed at each level [39, 40].

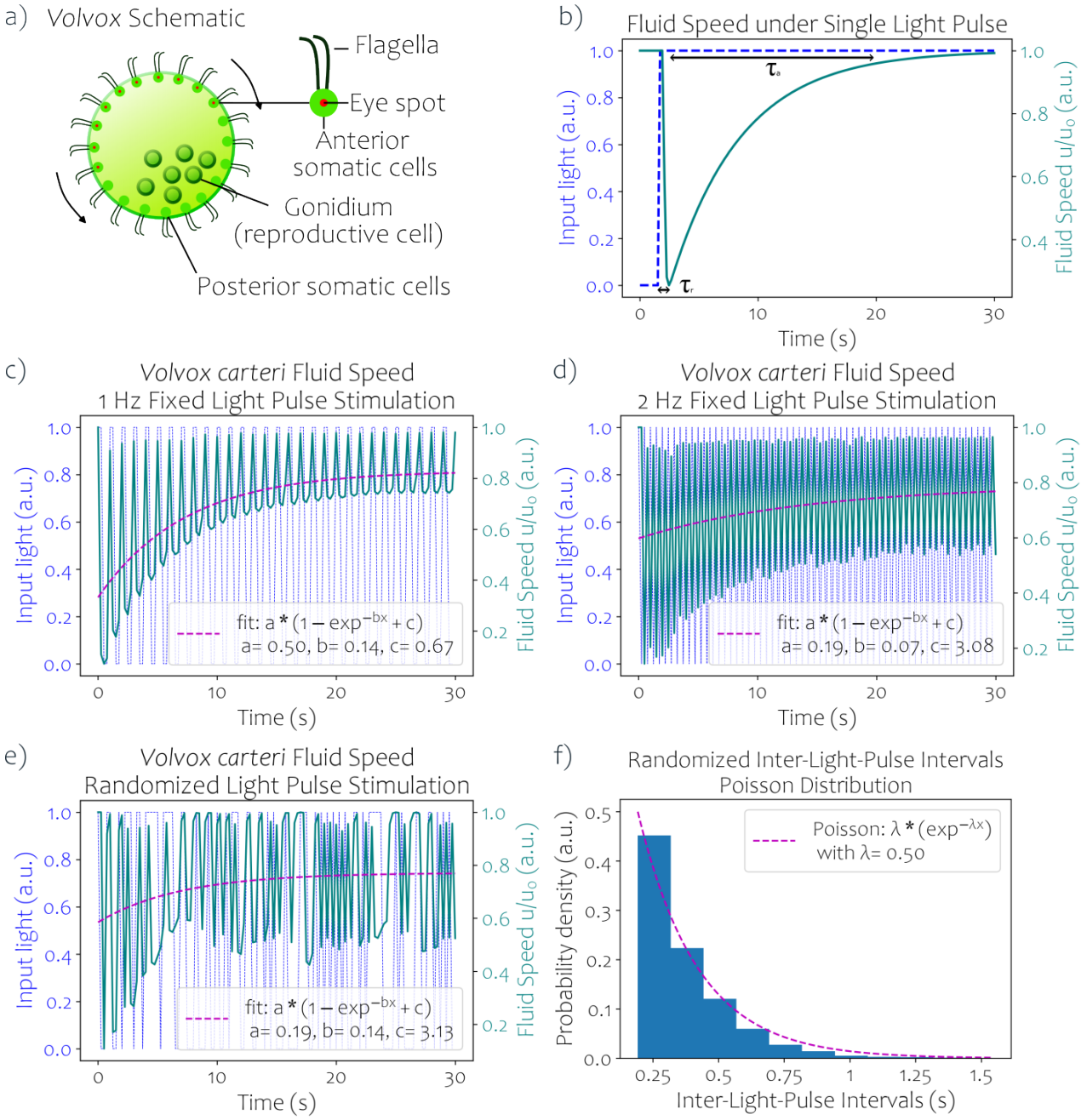

Figure 5. Simulation Predicts that Randomized Inputs Decrease Adaptive Phototactic Response in *Volvox*.

Volvox organismal colonies exhibit an adaptive response to light by virtue of their eyespots, which when stimulated by light downregulate flagellum beating speeds, resulting in biased movement towards the light. a) A schematic of *Volvox*. A *Volvox* organism (also called colony) consists of typically 5-10 reproductive cells in the interior, and up to 2000 vegetative cells on the exterior, each equipped with 2 flagella that exert net force around the *Volvox* colony towards the posterior side, moving it forwards through water. Anterior cells also possess an eyespot that allows light sensing. b) *In silico* modeling of *Volvox* photoadaptation (based on the equations from Drescher et al [15]). When a light stimulus is presented to a *Volvox* colony, eyespots, with higher deactivation strength in the anterior region of the *Volvox*, downregulate flagellum beating speed within a sub-second time window, which causes the organism to rotate and align its anterior-posterior axis with the direction of the input light. This adaptive downregulation of flagellum beating frequency is transient and recovers after a few seconds. Because of a slight torque in the *Volvox*, the organism can prevent misalignment by stabilizing this adaptive recovery period, exposing different eyespots to the light as the organism rotates

along its own axis. c-e) As simulation inputs, we used both fixed light pulse intervals with frequencies of 1 Hz (c) and 2 Hz (d), as well as randomized (e) pulse intervals with similar average interval length to stimulate flagellar beating downregulation over time. The average adaptive (or recovery) time (the time required for flagellar beating to return to baseline) is much longer for the randomized input, which is also quantified by fitting an exponential decay curve to the patterns. Specifically, variations around the fitted mean of the adaptive rate are increased over two-fold for the randomized sequence compared to the fixed pulse sequence, which would heavily interfere with correct colony orientation towards light. f) A computed histogram of the inter-light pulse intervals for the randomized stimulation sequences shows that they are Poisson distributed.

Since the ability of *Volvox* to maintain directionality in phototaxis is immensely time-constrained by their rotational frequency, which is closely matched with the photoresponse, we can hypothesize that a Poisson distributed light stimulation pattern will interfere with their ability to maintain their direction. This is because, by decreasing calcium signaling, such randomized activation patterns would effectively decouple colony rotation from photoactivation, whose evolved interdependency is at the heart of how *Volvox* maintain phototactic direction in the first place.

3.4 Temporal Selectivity of *Volvox* Photoadaptation is Altered by a Calcium Channel Blocker Targeting Primarily Internal Calcium Channels

We next investigated the mechanism underlying the temporal preferences we observed in phototactic outcomes both *in silico* and *in vivo*.

First, we characterized how components integral to the modularity of the adaptive photoresponse (*i.e.*, light activation and recovery time of downregulated flagellar beating speed) are implemented in *Volvox*. While initial calcium entry upon light activation occurs on the order of 19 milliseconds in this organism [41], its diffusion across the flagella has been estimated to take 0.2 seconds [15], a duration we can observe experimentally. We used nimodipine, a reagent commonly used to selectively inhibit calcium signaling [42, 43], and was previously shown in the close *Volvox* relative *Chlamydomonas* to bind to a calcium inhibitor binding protein localized primarily in the cell-internal membrane [44].

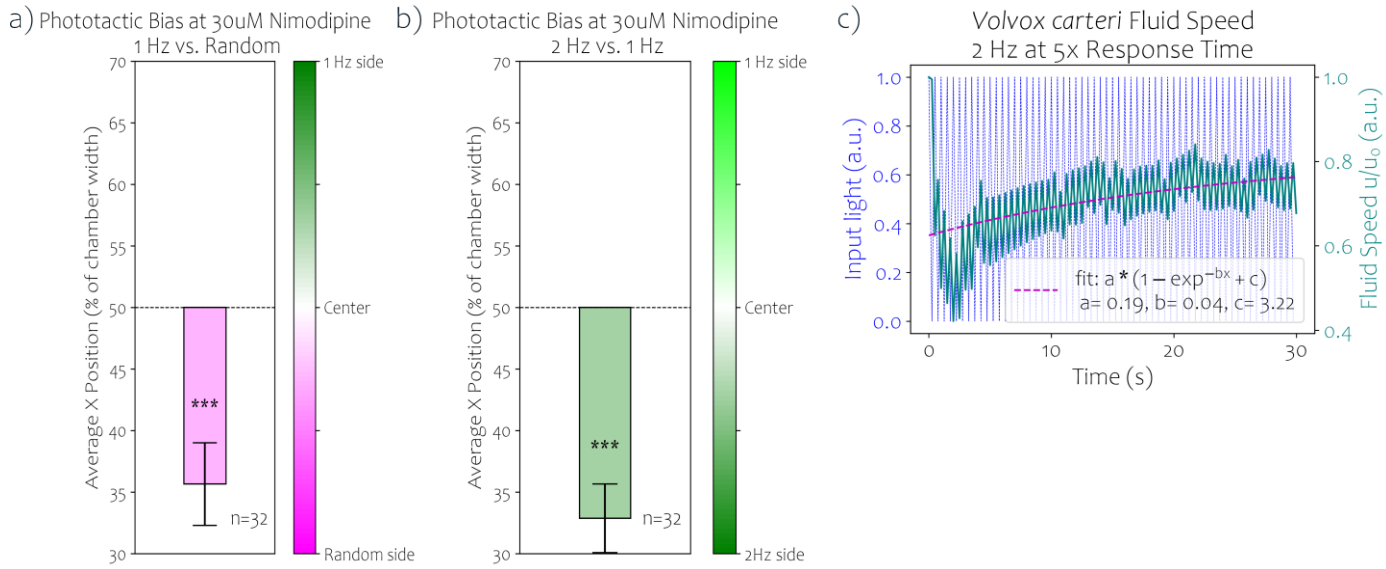

Figure 6. Calcium Flow Inhibitor Nimodipine Reverses 1 Hz to Random Bias and Induces 2 Hz to 1 Hz Bias.

Recording phototactic biases in *Volvox carteri* in the presence of 30 μM nimodipine revealed significant changes to phototactic biases. **a)** A very significant ($p<0.001$, Wilcoxon rank test) bias was observed towards the Random light side for nimodipine treated *Volvox*. **b)** Inhibition of calcium release and downstream diffusion along the flagella caused by nimodipine shifts phototactic preference to higher frequencies of 2 Hz, which was lacking in the *V. carteri* without the drug. **c)** Simulations of increased response time τ_r hypothesized to be caused by nimodipine show drastically lowered variations around the mean recovery rate plotted by the exponential decay fit normally induced by the high frequency rate as observed in Figure 5e.

This enabled us to observe the adaptive response of *Volvox* to light inputs in real time during inhibition of signaling from the photoreceptor to the flagella (Figure 6).

As blocking calcium this way slows down the calcium mediated signal progression from photoreceptor towards flagella and thereby causing a decrease in phototactic sensitivity [44], we can describe this effect in *Volvox* as an increase in the photoresponse time τ_r introduced earlier. Note that we shifted the speed filtering criteria for both normal and nimodipine containing media for lower speeds, as nimodipine also reduced overall speeds as a consequence of lowered phototactic sensitivity.

We tested whether such a decrease in internal calcium flow rates causes a shift in frequency dependence of phototactic preference. We found that in the presence of nimodipine, *Volvox* showed a significant phototactic bias towards the 2 Hz stimulus compared to the 1 Hz, while preference for the 1Hz regular stimulus compared to the random pulse sequence reversed. To explain this phenomenon, we turned back to the simulations from section 3.3, and simulated the fluid speed induced by flagellar

beating in response to the same 2Hz frequency as before, but this time, to simulate the effect of nimodipine, we increased response time τ_r by an arbitrary factor of 5 (exact value would need experimental validation through high speed imaging of flagellar activity and fluid flow in response to the drug).

We found that while the overall exponential fit was not too different from Figure 5e, the deceased response time reduces the overall amplitude of variation over the mean fluid response, making it more similar in shape to the regular step function. Using an analogy to human vision, this corresponds to shifting the high frequency light input below a flicker fusion rate (the rate at which an intermittent light stimulus is perceived as constant) the *Volvox* can perceive. While the response time was still reduced overall, the reduction in variations may mean there are fewer downstream influences that interfere with normal *Volvox* phototaxis. This suggests that inhibition of calcium release and diffusion shifts the sensed base frequency of the interval lengths that *Volvox* can perceive, akin to a flicker fusion rate in human vision, denoting a maximal light flickering frequency the human vision can no longer perceive as individual pulses.

3.5 *Volvox* Exhibit Memory Persistence Towards Past Light Direction

A necessary condition for pattern recognition and tracking over time is the persistence of a stimulus' effect on its internal state over a limited amount of time — a type of memory. To prove the existence of such a persistence of effect in *Volvox*, we designed an experiment to test if phototactic alignment of *Volvox* towards one stimulus persists after that stimulus ends. We used the experimental platform descried in Figure 1b and confined *Volvox aureus* into a 1 cm space at the center of the channel using transparent dividers and then illuminated them from one side with blue LED light for 5 minutes, after which we turned the light source off and allowed the *Volvox* colonies to travel freely for 10 minutes, collecting the *Volvox* at each section in the well as before. There was a significant ($p<0.05$, Wilcoxon signed-rank test) bias towards the previously illuminated side of the well, indicating persistence of phototactic alignment (Figure 7).

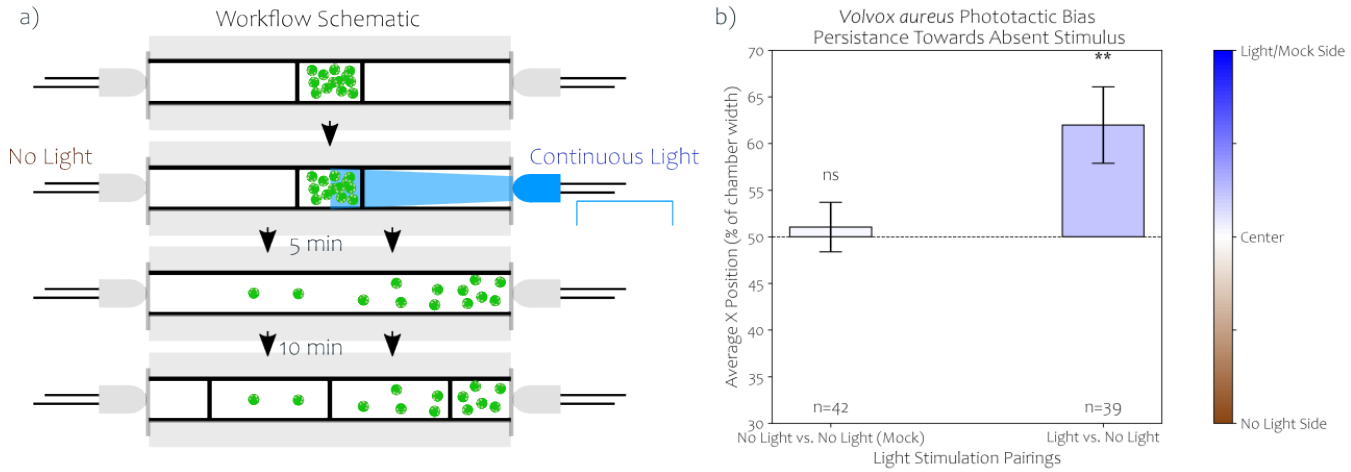

Figure 7. *Volvox* Phototactic Movement Persists for Minutes After Light Stimulus Ends.
a) Workflow schematic. *Volvox* were confined into a space of 1cm using transparent dividers and then illuminated from one side with blue LED light for 5 minutes, after which we turned the light source off and allowed the *Volvox* colonies to travel freely for 10 minutes, collecting the *Volvox* at each section in the well as before. **b)** A significant bias towards the previously illuminated side of the well was detected 10 minutes after light stimulus ended ($p<0.05$, Wilcoxon signed-rank test), indicating a persistence of phototactic alignment.

A likely mechanism of this persistence of effect is a sufficient combination of initial orientation of the *Volvox* colony towards light stimulus and a maintenance of that orientation over short time scales even in the presence of small-scale perturbations.

It is already known that the first part of that combination occurs: *Volvox* orient themselves towards light by virtue of the asymmetric distribution of photoreceptor activity along their sphere and flagellar orientation [15]. The fact that in our experiment, *Volvox* were still preferentially distributed towards the light stimulus ten minutes after it ends is evidence for the swimming orientation in *Volvox* being stabilized when a light stimulus is removed, which is why our result is a first evidence of short term memory in *Volvox*.

3.6 Photosynthesis Efficiency is Not Significantly Affected by Randomized Light Pulses Compared to the Fixed Frequency Light Stimulation Pattern

Next we wanted to find out whether *Volvox* photosynthesis was also affected by different light patterns, especially unpredictable ones, to test the hypothesis that the mechanism by which *Volvox* detect patterns vs. randomness involved monitoring of energy generation, and also whether such

patterned or random light stimulation would interfere with normal *Volvox* growth. We quantified photosynthetic efficiency using the *Firesting*™ (Pyrotechnics) to measure oxygen concentrations, using an external optical fiber probe to scan an oxygen-sensitive sensor inside glass vials containing *Volvox*. Because the individual sensors are highly sensitive to temperature and media conditions and are not stable in normal *Volvox* culturing conditions over longer times, we were limited to taking measurements at individual timepoints and used a temperature probe inside the vial for temperature compensation. Measuring oxygen concentrations at two timepoints per day, one in the morning and one in the evening, we observed that oxygen levels in the media rose significantly in the continuous light treatment (our positive control) but not in either the randomized light pulse group, or the fixed light pulse series treatment (our negative control).

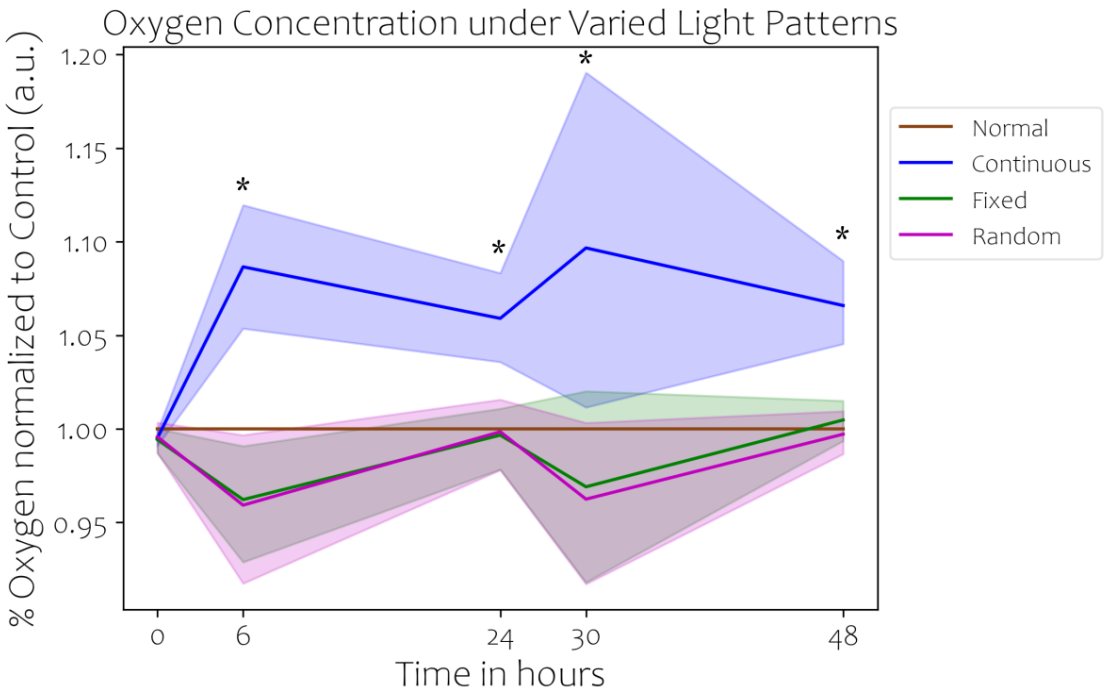

Figure 8. Regular and Randomized pulsed light Does Not Increase Oxygen Concentrations in *Volvox* media.
Line plots of percent oxygen concentrations over time for each group normalized to that of a control group from the same culture stock maintained in normal incubator conditions. As expected, the positive control – continuous light treatment (slightly higher light density exposure than provided by the normal incubator lights) - significantly increased oxygen concentration in the medium.

Because in both experimental conditions, the light was off for 50% of the exposure, we expected a significant decrease in photosynthesis, which was however not detectable with the statistical power of our experiment. The lack of significant difference between the fixed and random light pulse conditions suggests that random pattern avoidance in *Volvox* did not evolve simply to maximize energy but is instead a core feature of the way they process their environment.

3.7 *Volvox* Adapt to Long Term Exposure of Patterned Culture Light

We next wanted to investigate the ability of *Volvox* to adapt in the long term, rather than just in the short term as above, to the same patterned and random light conditions in their culturing environment in time frames close to evolutionary time scales. We asked whether *Volvox* would adjust their preferences in the long-term, by exposing *Volvox* to the different light conditions for 2 years and then remeasuring their phototactic biases as above.

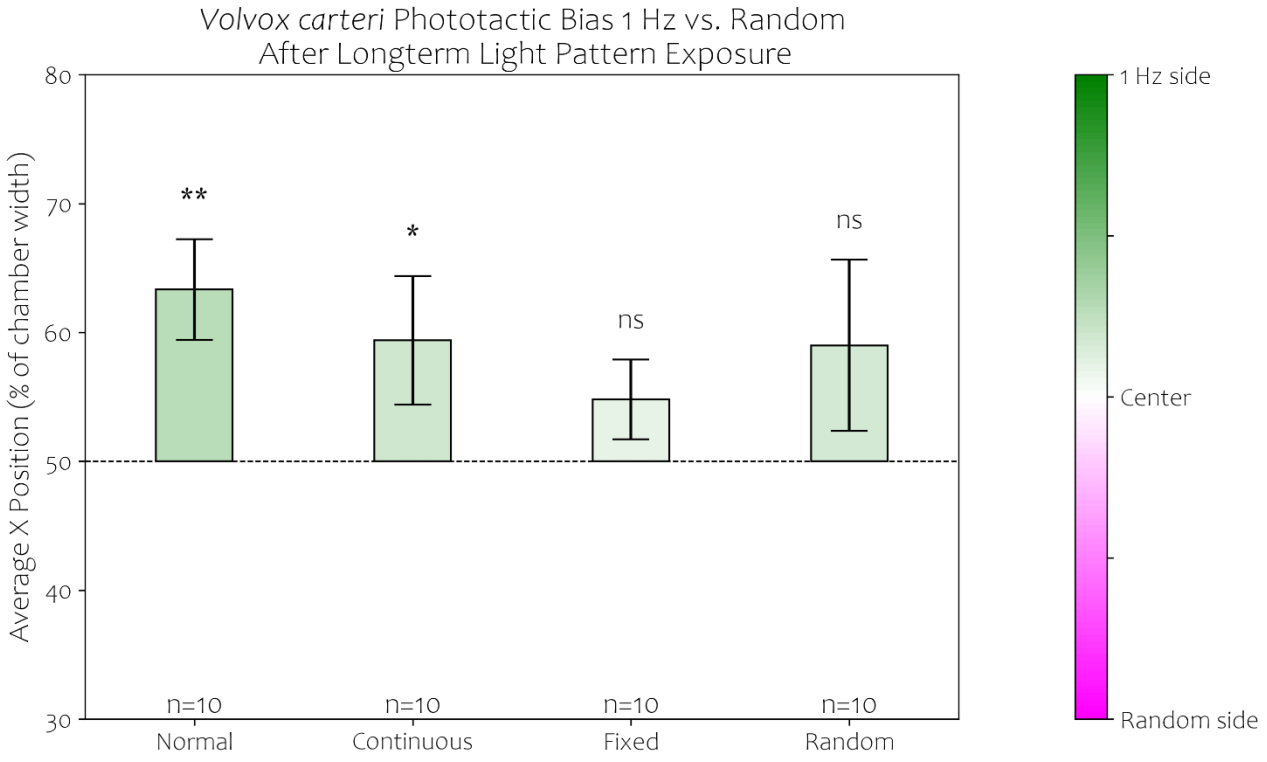

Figure 9. Long Term Light Pattern Exposed *Volvox* Lose Phototactic Biases Against Random Light Stimulation.
Volvox exposed to randomized and 1 Hz light pulse frequency no longer exhibit a phototactic bias towards the 1 Hz stimulus side. This indicates a habituation to the patterned light pulse series in both cases.

The result was that *Volvox* exposed to either, randomized or 1 Hz light pulse frequency, no longer exhibited a phototactic bias towards the 1 Hz stimulus side (see Figure 9a). This change was not however accompanied by a shift in biases between 1 Hz and 2 Hz stimuli, as differences in biases in these graphs remained non-significant (see Figure 9b).

This remarkable finding takes the short-term adaptation of the earlier sections on phototactic biases and short-term memory (all in the scale of minutes) to much more long term changes at the population level in the order of months to years.

3.8 Patterned Electric Shocks Interfere with Photoadaptation

Next, we examined the effect of a different kind of uncertainty-induced stress on photoadaptation. Unpredictable electric shocks have been widely used to increase stress in neural organisms experimentally. A 2016 study in human participants by Berker *et al*. found high correlation between stress responses, measured through physiological changes including pupil diameter and skin conductance, and environmental uncertainty [45]. Linking stress and uncertainty from the external environment could help organisms more quickly adapt to their changing environments providing an advantage both during the organism's lifetime and evolutionarily. However, increased stress as a response to unpredictable environmental stimuli has not been studied much in simpler, aneural organisms, particularly when light and electricity are used as the stimuli.

To assess the effect of random electric shocks on photoadaptation, we used a 30mm chamber in which the light axis and electric current axis were perpendicularly paired. Dynamic lights were used with the light source switching between the top and bottom of the chamber every 60 seconds. The top lights were engaged for 60 seconds and then completely turned off while the bottom lights were on for 60 seconds. The switching lights provided more opportunities to observe phototactic behavior and ensured that *Volvox* would not be directed towards and get stuck at one side. To ensure that there was no physical bias, the stage holding the chamber was leveled and the light intensity of each LED was measured and adjusted to achieve equal brightness output for the top and bottom lights.

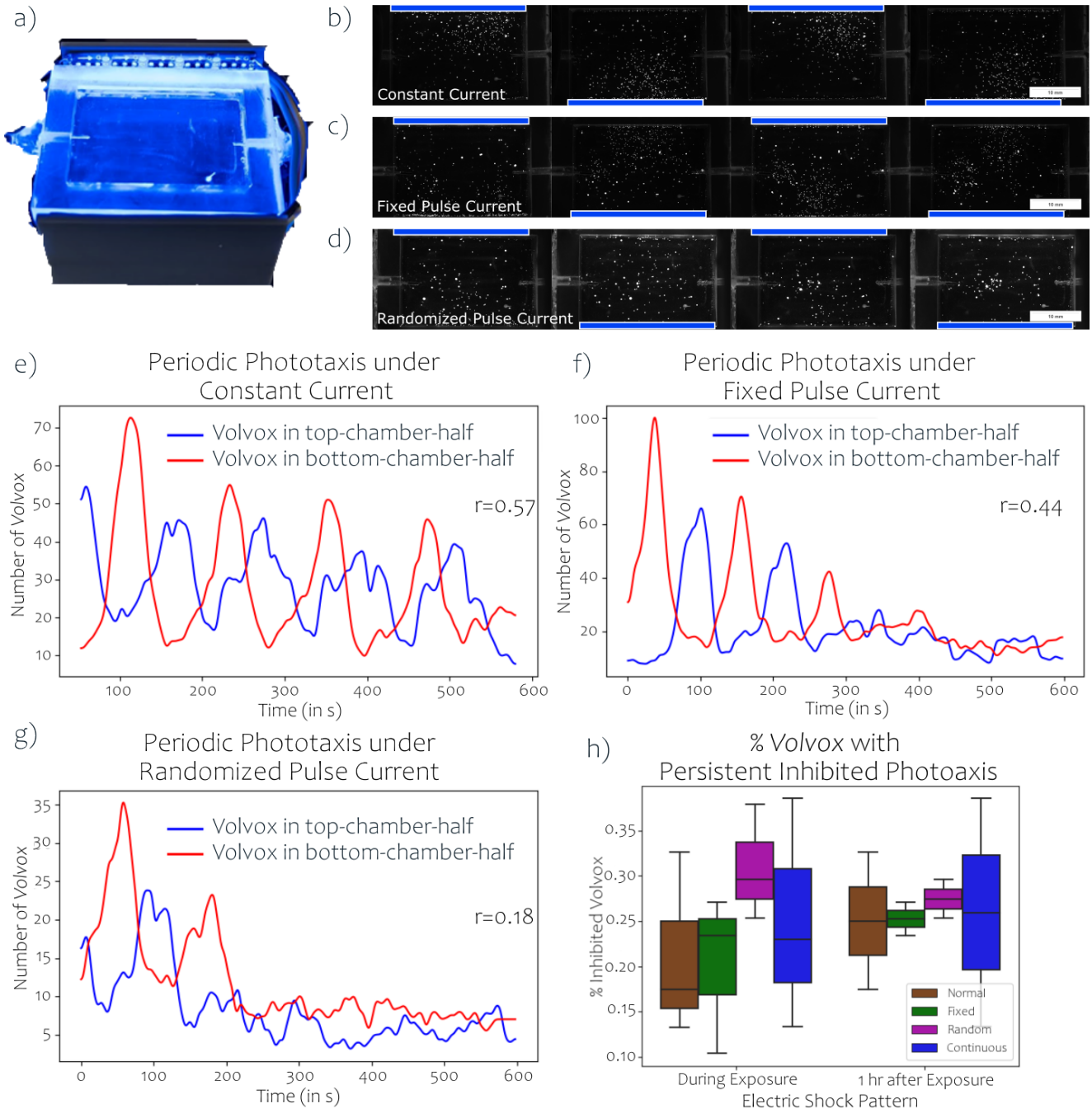

Figure 10. Pulsed Electric Shock Inhibits Adaptive Phototaxis.
a) Larger *Volvox* chamber with platinum electrodes for simultaneous stimulation through electric current and light. b-c) Montage of *Volvox* localization following oscillating dynamic light source, under continuous (top), fixed (middle) and randomized (bottom) pulse sequenced electric shocks. Blue bars show the light source in each time frame. e-g) Quantification of number of *Volvox* in each half of the chamber (blue and red lines show the number of *Volvox* in the chamber close to the top and bottom light sources, respectively.) While photoadaptation under constant current was slightly attenuated over time, but otherwise largely intact (e), it declines sooner under fixed shock pulse sequence (f), and even more rapidly under a randomized pulse sequence (g). h) Effect of treatment on *Volvox* motility. We counted the number of *Volvox* that were no longer exhibiting any kind of motion at the end of the 30-minute treatment and one hour later in 3 replicates each, as an indicator of overall health and found no detectable statistically significant reduction of motility over time between any of the electric shock treatment groups (2-way ANOVA).

When current was applied to the chamber in a continuous fashion, *Volvox* colonies exhibited consistent phototactic behavior over the course of the whole ten minutes. The *Volvox* colonies started moving towards the light source strongly as seen by the increase in *Volvox* in the top quartile.

As the light source location changed, the *Volvox* then moved more towards the bottom, as seen by the decrease in *Volvox* in the top quartile and an increase in the number of *Volvox* in the bottom quartile. While the number of *Volvox* in the top of the chamber peaked at 100 seconds, and then declined slightly, phototaxis clearly continued throughout the treatment.

We next exposed *Volvox* to dynamic light stimuli and fixed frequencies of electric current. At first, the behavior was similar to that seen with continuous current; however, after 150 seconds there was a large drop in the maximum number of *Volvox* able to move back to the top of the chamber. This indicates that the fixed pulses of current hinder *Volvox* phototaxis compared to continual exposure to electricity. The reduction in phototaxis was gradual but clear towards the end of the experiment, when most *Volvox* are distributed equally throughout each quadrant, indicating that the *Volvox* are not localized to any particular side over time and are hence moving less.

Finally, new *Volvox* were subjected to random pulses of current while exposed to a switching light source. Randomized current pulses interrupted phototactic behavior much more quickly (at about 225 seconds compared to > 325 seconds for the fixed current pulses, while continuous current exposure did not exhibit a clear phototactic interruption point.) Interestingly, in neurons, repetitive application of electric shock pulses can cause progressive but reversible decrease in spontaneous depolarizing potentials [46]. While the channelrhodopsin protein responsible for light sensing and downstream calcium flow into flagella is not directly voltage gated, a similar mechanism could affect its spontaneous ability to open in response to light, but this would need to be studied further in future studies.

4 Discussion and Conclusions

We have shown through the phototactic biases observed in *Volvox* to more regular light pulse patterns and our extensive manipulation thereof, how irregular, unpredictable signaling activation leads to a reduced capability of simple cognitive systems to perform variational free energy minimization and hence correctly infer and perform correct action-perception.

Using the example of the green algae *Volvox*, we have provided a minimalistic realization of physiological equations that govern the inherent pattern recognition and surprise minimization realized by the phototaxis adaptive response. This adaptive response was shown not just to be input frequency dependent but was also capable of differentiating a more regular from an irregular input modulation. Furthermore, by employing two different species of *Volvox* in our experimental approach, who are evolutionary very close to each other (about 75 million years of evolutionary distance [36]), we were able to show that while small variations in phototactic preferences towards different light pulse frequencies were present, preference towards regular over irregular patterns were present in both species, further underlying our claim about the ubiquitousness of uncertainty minimization.

The significant variance across individuals that we observed for both species most likely stems from a combination of (to a lesser extent) remaining light artifacts of non-parallel illumination, and (to a higher extent) initial distribution of sizes and random starting positions. Moreover, variances between individual *Volvox* size and age (in terms of their stage in their lifecycle), health, eccentricity (how much they deviate from a perfect spherical shape that influences their tumbling and hence fidelity of their phototactic behavior) and any possible flagellar patterning aberrations (stemming from slight deviations from ideal morphogenetic processes, which would also affect their tumbling), are all likely to introduce variations in their ability to react and move towards different light patterns as predicted. Lastly, any significant biochemical variations between *Volvox*, such as for example internal calcium storages and channelrhodopsin excitability, would also affect the speed and duration of their photoadaptive machinery and would in turn shift any phototactic biases as well.

By elucidating the mechanism that governs the physiological response variables through calcium in *Volvox*, we have shown how a system is fine-tuned to certain expected signals in terms of its characteristic response and adaptive time constants setting the perception limits of individual stimulation pulses. Based on abstract uncertainty minimization alone without any mechanistic underpinning alone, we would have predicted that nimodipine should not change the preference to a patterned vs. a randomized input; however, that bias is likely substantially hidden here because of the modulation of frequency response by nimodipine. This is analogous to the reason that white noise does not illicit a strong aversion or stress response in humans unless at high decibels: despite its highly random nature, the randomly distributed frequencies are too high to be perceived by human brains as individual pulses, but instead blend together as a background that can even be soothing to infants [47], or help with concentration by tuning out more perceivable randomly occurring acoustic events in the environment [48]. In addition to specific mechanistic insight into photoadaptation in *Volvox,* these findings will provide insight into how the minimization of variational free energy at the root of surprise minimization [20] is implemented mechanistically in an organism with a simple behavior, equipping us with the knowledge and tools needed to look for similar behavioral modes in other systems and to manipulate them.

We also showed that direct metabolic function of *Volvox* in terms of photosynthetic output appears to be largely unaffected by light pattern recognition through the observed phototactic biases observed throughout this work, as the patterned light treatment groups did not show statistically significant decreases in oxygen concentration within the statistical power of this experiment. Any trend that we saw her in terms of slightly lower oxygen concentration in the Random group would have to be extended in future experiments under longer time frames that carefully observe and control for difference in colony and population growth that could be obscuring those trends in our current results. As it stands, this is evidence supporting the notion that any long-term adaptive response by *Volvox* to light patterns is also not driven by a purely energy-based selection pressure. While evolutionary principles

inevitably apply here too, the selection pressure would appear to be more nuanced than simply a question of which light pattern yields the highest photosynthetic yield.

Future work could more explicitly investigate whether it is possible to introduce strong biases in phototaxis towards a more predictable pattern that however yields lower photosynthetic outcomes, which would be evidence for proto-cognitive/informational considerations overriding metabolic imperatives. This would support the argument that informational concerns need to be more explicitly addressed in evolutionary approaches [27, 31].

Throughout this work, we referred to the short-term changes in light sensitivity in the eyespot and downstream flagellar beating responsivity in *Volvox* that are the core of their ability to orient themselves towards light and maintain direction as *photoadaptation*, as has been in previous studies [15]. This notation aligns well with how adaptation is used in neuroscience, specifically when referring to the visual system. Short-term processes like visual reduction or increase of light sensitivity to changing light conditions are referred to as adaptive [49]. Indeed, short term synaptic depression, which is very similar to what we observe here, is the central part of these adaptive responses [50] and is the precursor to long term depression (LTD) that underlies learning in neural systems together with its opposite, long term potentiation (LTP).

Interestingly, although constant-frequency stimulation trains are the standard stimulation method for many experimental studies on synaptic plasticty, they are unlikely to be experienced by neurons in a real brain, where inputs tend to be much more irregular [37]. In fact, the Poission distribution that best describes our randomized light pulse stimulation is also one of most representative stimulation patterns in brains *in vivo* [37]. Given the common evolutionary ancestry of the voltage-gated ion channels in neurons and the light-gated ion channels controlling flagellar motion in *Volvox*, we considered how the inter-light pulse dependency of photoadaptation *in Volvox* may be related to spike timing dependent plasticity (STDP) in neurons. STDP refers to the finding that the sign and magnitude of changes in neuronal synaptic strength (a foundation of learning in neural networks) depend on the precise timing of action potential spikes in the stimulus [38].

Additional parallels to the calcium mediated response in *Volvox* may be indicated by the fact that synaptic signal transmnission is also highly modulated by dynamic calcium fluxes. In addition to its dependence on stimulus timing, Hata *et al.* examined, *in silico,* the critical role of post-synaptic Ca^{2+} flux in synaptic modulation [37]. Changing the post-synaptic neuron's calcium decay constant from 40 ms to 80 ms switches the effect of stimulation with Poisson-distributed activity between the two most fundamental changes to synaptic strength that underlie all learning processes, LTD and LTP. When the postsynaptic neuron's calcium decay constant is 80ms, the stimulus results in long-term potentiation; if it is 40 ms, the same stimulus results in long-term depression [37]. Hata *et al.* also showed that postsynaptic calcium levels were reduced for poisson-distributed inter-spike distances compared to fixed frequency spike trains. This finding is particularly relevant to the photoresponse in *Volvox*, as its calcium-dependent ion channels propagate the response from the photoreceptor (which is channel rhodopsin mediated) to the flagellum, downregulating flagellar beating frequency and hence determining fluid speed on the *Volvox* colony surface [41]. Calcium activity in the *Volvox* photoresponse is largly dependent on two time scales: the initiation of a calcium current is on the order of 1ms, while the diffusion of calcium along the flagellum is on the order of 200ms [15].

In addition, we have proven the existence of basic memory in phototactic alignment in *Volvox* as a necessary condition for pattern recognition and temporal stimulus tracking. By persisting on phototactic trajectories set in past light stimuli, *Volvox* have at least one of two major necessary components for learning: memory and plasticity. One can speculate that this behavior evolved to maintain phototactic orientation when momentarily exposed to shadows, which would be a very clear illustration of why memory and learning could evolve even in such low complexity organism. Indeed, research by Mast *et al.* showed that upon drastic decrease of light stimulus, *Volvox* exhibit reduced rotational speed and hence faster forward movement [51], thereby stabilizing directed movement toward the light during short periods of light obstruction.

Finally, we have shown that *Volvox* can adapt over time to light patterns which they seem to avoid due to their unpredictability, laying the groundwork for studying evolution of specific, temporally fine-

tuned adaptive responses in simple organisms. This finding also suggests that *Volvox* exhibit plasticity in their behavior in response to the information content of their environment, as represented by the pattern recognition mode we tested throughout this work. While detailed molecular analyses need to be performed on the makeup of these phototactic changes in future work, this is a clear indication that pattern recognition can lead to long-term changes in aneural organism and even potentially be a drive for evolutionary change as we have previously hypothesized [27]. The fully-annotated genome of *V. carteri* will allow us to examine transcriptional responses as part the photoadaptive response. For example, through ubiquitous cellular stress response pathways such as heath shock proteins we could test whether unsuccessful uncertainty minimization (in response to the randomized stimuli in our experiments) would be accompanied by higher amounts of stress in algae in a similar manner as observed in humans [45].

In future work, the bridging between physiological differential equations governing adaptive responses and information processing, predictive-coding-based approaches such as the free energy principle needs to be made explicit into one combined framework. Fundamentally, the ability to distinguish regular vs. random stimuli requires the agent to detect a pattern, which in turn can be used as a kind of IQ test; how complex of a pattern can *Volvox* (or any other unconventional model system) detect and distinguish from randomness? This will be determined in future work. Such assays, in molecularly-tractable living systems, offer the possibility of understanding memory, learning, and intelligence across a very wide range of substrates [52-57] — a possibility that may have considerable implications for biomedicine, exobiology, and synthetic morphoengineering [58, 59]. Equipped with explicit, mechanistic implementations of surprise minimization, we could achieve unprecedented rational control over cellular function and organismal behavior that would not necessitate rewriting the internal model of a cell (such as its DNA through gene therapy). Instead, it would rely on fine spatio-temporal control of the environmental signals an organism receives, allowing us to build on many recent biotechnological breakthroughs, such as optogenetics, to study and take advantage of the many unexpected competencies of our biological materials [59, 60].

Acknowledgements:

We thank the Olson lab, Bradley Olson and Berenice Jiménez-Marín in particular, for providing the *Volvox carteri* strains and guidance on culture maintenance. We also thank Dimitri Kromm, Juanita Mathews, and Wesley Clawson for their comments in this manuscript and, together with Devon Davidian, for helpful discussions and advice on experimental techniques. We also thank Karl Friston for his guidance and scientific body of work that inspired the approach in this manuscript. M.L. gratefully acknowledges support via Grant 62212 from the John Templeton Foundation. The opinions expressed in this publication are those of the author(s) and do not necessarily reflect the views of the John Templeton Foundation.

5 References

[1] Baluska, F. & Levin, M. 2016 On Having No Head: Cognition throughout Biological Systems. *Front Psychol* **7**, 902. (DOI:10.3389/fpsyg.2016.00902).

[2] Lyon, P. 2006 The biogenic approach to cognition. *Cogn Process* **7**, 11-29. (DOI:10.1007/s10339-005-0016-8).

[3] Lyon, P. 2015 The cognitive cell: bacterial behavior reconsidered. *Front Microbiol* **6**, 264. (DOI:10.3389/fmicb.2015.00264).

[4] Jennings, H. S. 1931 *Behavior of the lower organisms*, Columbia University Press.

[5] Losick, R. M. 2020 Bacillus subtilis: a bacterium for all seasons. *Curr Biol* **30**, R1146-R1150. (DOI:10.1016/j.cub.2020.06.083).

[6] Thiery, S. & Kaimer, C. 2020 The Predation Strategy of Myxococcus xanthus. *Front Microbiol* **11**, 2. (DOI:10.3389/fmicb.2020.00002).

[7] Wolf, D. M., Fontaine-Bodin, L., Bischofs, I., Price, G., Keasling, J. & Arkin, A. P. 2008 Memory in microbes: quantifying history-dependent behavior in a bacterium. *PLoS One* **3**, e1700. (DOI:10.1371/journal.pone.0001700).

[8] Tagkopoulos, I., Liu, Y. C. & Tavazoie, S. 2008 Predictive behavior within microbial genetic networks. *Science* **320**, 1313-1317. (DOI:10.1126/science.1154456).

[9] Murugan, N. J., Kaltman, D. H., Jin, P. H., Chien, M., Martinez, R., Nguyen, C. Q., Kane, A., Novak, R., Ingber, D. E. & Levin, M. 2021 Mechanosensation Mediates Long-Range Spatial Decision-Making in an Aneural Organism. *Adv Mater* **33**, e2008161. (DOI:10.1002/adma.202008161).

[10] Shirakawa, T., Gunji, Y.-P. & Miyake, Y. 2011 An associative learning experiment using the plasmodium of Physarum polycephalum. *Nano Communication Networks* **2**, 99-105. (DOI:10.1016/j.nancom.2011.05.002).

[11] Allan, C., Morris, R. J. & Meisrimler, C. N. 2022 Encoding, transmission, decoding, and specificity of calcium signals in plants. *J Exp Bot* **73**, 3372-3385. (DOI:10.1093/jxb/erac105).

[12] Baluska, F. & Mancuso, S. 2021 Individuality, self and sociality of vascular plants. *Philos Trans R Soc Lond B Biol Sci* **376**, 20190760. (DOI:10.1098/rstb.2019.0760).

[13] Beilby, M. J. 2007 Action potential in charophytes. *Int Rev Cytol* **257**, 43-82. (DOI:10.1016/S0074-7696(07)57002-6).

[14] Appel, H. M. & Cocroft, R. B. 2014 Plants respond to leaf vibrations caused by insect herbivore chewing. *Oecologia* **175**, 1257-1266. (DOI:10.1007/s00442-014-2995-6).

[15] Drescher, K., Goldstein, R. E. & Tuval, I. 2010 Fidelity of adaptive phototaxis. *Proc Natl Acad Sci U S A* **107**, 11171-11176. (DOI:10.1073/pnas.1000901107).

[16] Mitchell, A., Wei, P. & Lim, W. A. 2015 Oscillatory stress stimulation uncovers an Achilles' heel of the yeast MAPK signaling network. *Science* **350**, 1379-1383. (DOI:10.1126/science.aab0892).

[17] Bugaj, L. J., O'Donoghue, G. P. & Lim, W. A. 2017 Interrogating cellular perception and decision making with optogenetic tools. *J Cell Biol* **216**, 25-28. (DOI:10.1083/jcb.201612094).

[18] Toettcher, J. E., Weiner, O. D. & Lim, W. A. 2013 Using optogenetics to interrogate the dynamic control of signal transmission by the Ras/Erk module. *Cell* **155**, 1422-1434. (DOI:10.1016/j.cell.2013.11.004).

[19] Wilson, M. Z., Ravindran, P. T., Lim, W. A. & Toettcher, J. E. 2017 Tracing Information Flow from Erk to Target Gene Induction Reveals Mechanisms of Dynamic and Combinatorial Control. *Mol Cell* **67**, 757-769 e755. (DOI:10.1016/j.molcel.2017.07.016).

[20] Kuchling, F., Friston, K., Georgiev, G. & Levin, M. 2019 Morphogenesis as Bayesian inference: A variational approach to pattern formation and control in complex biological systems. *Physics of life reviews*.

[21] Pezzulo, G., Cartoni, E., Rigoli, F., Pio-Lopez, L. & Friston, K. 2016 Active Inference, epistemic value, and vicarious trial and error. *Learn Mem* **23**, 322-338. (DOI:10.1101/lm.041780.116).

[22] Friston, K. 2013 Life as we know it. *J R Soc Interface* **10**, 20130475. (DOI:10.1098/rsif.2013.0475).

[23] Pezzulo, G., Parr, T. & Friston, K. 2022 The evolution of brain architectures for predictive coding and active inference. *Philos Trans R Soc Lond B Biol Sci* **377**, 20200531. (DOI:10.1098/rstb.2020.0531).

[24] Friston, K., Levin, M., Sengupta, B. & Pezzulo, G. 2015 Knowing one's place: a free-energy approach to pattern regulation. *J R Soc Interface* **12**. (DOI:10.1098/rsif.2014.1383).

[25] Chater, N., Oaksford, M., Hahn, U. & Heit, E. 2010 Bayesian models of cognition. *WIREs Cognitive Science* **1**, 811-823. (DOI:10.1002/wcs.79).

[26] Colas, F., Diard, J. & Bessière, P. 2010 Common Bayesian Models for Common Cognitive Issues. *Acta Biotheoretica* **58**, 191-216. (DOI:10.1007/s10441-010-9101-1).

[27] Kuchling, F., Fields, C. & Levin, M. 2022 Metacognition as a Consequence of Competing Evolutionary Time Scales. *Entropy (Basel)* **24**, 601. (DOI:10.3390/e24050601).

[28] Lyon, P. & Kuchling, F. 2021 Valuing what happens: a biogenic approach to valence and (potentially) affect. *Philos Trans R Soc Lond B Biol Sci* **376**, 20190752. (DOI:10.1098/rstb.2019.0752).

[29] Karl, F. 2012 A Free Energy Principle for Biological Systems. *Entropy (Basel)* **14**, 2100-2121. (DOI:10.3390/e14112100).

[30] Kirchhoff, M., Parr, T., Palacios, E., Friston, K. & Kiverstein, J. 2018 The Markov blankets of life: autonomy, active inference and the free energy principle. *J R Soc Interface* **15**. (DOI:10.1098/rsif.2017.0792).

[31] Campbell, J. O. 2016 Universal Darwinism As a Process of Bayesian Inference. *Front Syst Neurosci* **10**, 49. (DOI:10.3389/fnsys.2016.00049).

[32] Keijzer, F., van Duijn, M. & Lyon, P. 2013 What nervous systems do: early evolution, input-output, and the skin brain thesis. *Adapt Behav* **21**, 67-85. (DOI:Doi 10.1177/1059712312465330).

[33] Fields, C., Bischof, J. & Levin, M. 2020 Morphological Coordination: A Common Ancestral Function Unifying Neural and Non-Neural Signaling. *Physiology* **35**, 16-30. (DOI:10.1152/physiol.00027.2019).

[34] Frank, T. D. 2012 Multistable Pattern Formation Systems: Candidates for Physical Intelligence? *Ecological Psychology* **24**, 220 - 240.

[35] Stasenko, S., Telnykh, A., Shemagina, O., Nuidel, I., Kovalchuk, A. & Yakhno, V. 2022 Biomorphic artificial intelligence system for pattern recognition problems with adaptive error correction. In *2022 Fourth International Conference Neurotechnologies and Neurointerfaces (CNN)* (pp. 185-189.

[36] Herron, M. D. 2016 Origins of multicellular complexity: Volvox and the volvocine algae. *Mol Ecol* **25**, 1213-1223. (DOI:10.1111/mec.13551).

[37] Hata, K., Araki, O., Yokoi, O., Kusakabe, T., Yamamoto, Y., Ito, S. & Nikuni, T. 2020 Multicoding in neural information transfer suggested by mathematical analysis of the frequency-dependent synaptic plasticity in vivo. *Sci Rep* **10**, 13974. (DOI:10.1038/s41598-020-70876-4).

[38] Shouval, H. Z., Wang, S. S. & Wittenberg, G. M. 2010 Spike timing dependent plasticity: a consequence of more fundamental learning rules. *Front Comput Neurosci* **4**. (DOI:10.3389/fncom.2010.00019).

[39] Amarasingham, A., Chen, T.-L., Geman, S., Harrison, M. T. & Sheinberg, D. L. 2006 Spike Count Reliability and the Poisson Hypothesis. *The Journal of Neuroscience* **26**, 801-809. (DOI:10.1523/jneurosci.2948-05.2006).

[40] Wiener, M. C. & Richmond, B. J. 2003 Decoding Spike Trains Instant by Instant Using Order Statistics and the Mixture-of-Poissons Model. *The Journal of Neuroscience* **23**, 2394-2406. (DOI:10.1523/jneurosci.23-06-02394.2003).

[41] Braun, F. J. & Hegemann, P. 1999 Two light-activated conductances in the eye of the green alga Volvox carteri. *Biophys J* **76**, 1668-1678. (DOI:10.1016/S0006-3495(99)77326-1).

[42] Nelson, M. T. & Worley, J. F. 1989 Dihydropyridine Inhibition of Single Calcium Channels and Contraction in Rabbit Mesenteric Artery Depends on Voltage. *The Journal of Physiology* **412**, 65-91. (DOI:10.1113/jphysiol.1989.sp017604).

[43] Akaike, N., Kostyuk, P. G. & Osipchuk, Y. V. 1989 Dihydropyridine-sensitive Low-threshold Calcium Channels in Isolated Rat Hypothalamic Neurones. *The Journal of Physiology* **412**, 181-195. (DOI:10.1113/jphysiol.1989.sp017610).

[44] Hegemann, P., Neumeier, K., Hegemann, U. & Kuehnle, E. 1990 The role of calcium in Chlamydomonas photomovement responses as analysed by calcium channel inhibitors. *Photochem Photobiol* **52**, 575-583. (DOI:10.1111/j.1751-1097.1990.tb01802.x).

[45] de Berker, A. O., Rutledge, R. B., Mathys, C., Marshall, L., Cross, G. F., Dolan, R. J. & Bestmann, S. 2016 Computations of uncertainty mediate acute stress responses in humans. *Nat Commun* **7**, 10996. (DOI:10.1038/ncomms10996).

[46] Calabresi, P., Mercuri, N. B., Stefani, A. & Bernardi, G. 1990 Synaptic and intrinsic control of membrane excitability of neostriatal neurons. I. An in vivo analysis. *Journal of neurophysiology* **63**, 651-662. (DOI:10.1152/jn.1990.63.4.651).

[47] Karakoc, A. & Turker, F. 2014 Effects of white noise and holding on pain perception in newborns. *Pain Manag Nurs* **15**, 864-870. (DOI:10.1016/j.pmn.2014.01.002).

[48] Awada, M., Becerik-Gerber, B., Lucas, G. & Roll, S. 2022 Cognitive performance, creativity and stress levels of neurotypical young adults under different white noise levels. *Sci Rep* **12**, 14566. (DOI:10.1038/s41598-022-18862-w).

[49] Kohn, A. 2007 Visual adaptation: physiology, mechanisms, and functional benefits. *Journal of neurophysiology* **97**, 3155-3164. (DOI:10.1152/jn.00086.2007).

[50] Chance, F. S., Nelson, S. B. & Abbott, L. F. 1998 Synaptic depression and the temporal response characteristics of V1 cells. *J Neurosci* **18**, 4785-4799. (DOI:10.1523/JNEUROSCI.18-12-04785.1998).

[51] Mast, S. O. 1926 Reactions to light in Volvox, with special reference to the process of orientation. *Zeitschrift f□r Vergleichende Physiologie* **4**, 637-658. (DOI:10.1007/bf00342378).

[52] Katz, Y. & Fontana, W. 2022 Probabilistic Inference with Polymerizing Biochemical Circuits. *Entropy (Basel)* **24**. (DOI:10.3390/e24050629).

[53] Katz, Y., Springer, M. & Fontana, W. 2018 Embodying probabilistic inference in biochemical circuits. (p. arXiv:1806.10161.

[54] Katz, Y., Goodman, N. D., Kersting, K., Kemp, C. & Tenenbaum, J. B. 2018 Modeling Semantic Cognition as Logical Dimensionality Reduction. In *Proceedings of Thirtieth Annual Conference of the Cognitive Science Society* (

[55] Katz, Y. & Springer, M. 2016 Probabilistic adaptation in changing microbial environments. *PeerJ* **4**, e2716. (DOI:10.7717/peerj.2716).

[56] Biswas, S., Clawson, W. & Levin, M. 2022 Learning in Transcriptional Network Models: Computational Discovery of Pathway-Level Memory and Effective Interventions. *Int J Mol Sci* **24**. (DOI:10.3390/ijms24010285).

[57] Biswas, S., Manicka, S., Hoel, E. & Levin, M. 2021 Gene Regulatory Networks Exhibit Several Kinds of Memory: Quantification of Memory in Biological and Random Transcriptional Networks. *iScience* **24**, 102131. (DOI:https://doi.org/10.1016/j.isci.2021.102131).

[58] Lagasse, E. & Levin, M. 2023 Future medicine: from molecular pathways to the collective intelligence of the body. *Trends Mol Med*. (DOI:10.1016/j.molmed.2023.06.007).

[59] Davies, J. & Levin, M. 2023 Synthetic morphology with agential materials. *Nature Reviews Bioengineering* **1**, 46-59. (DOI:10.31219/osf.io/xrv8h).

[60] Pezzulo, G. & Levin, M. 2015 Re-membering the body: applications of computational neuroscience to the top-down control of regeneration of limbs and other complex organs. *Integr Biol (Camb)* **7**, 1487-1517. (DOI:10.1039/c5ib00221d).